https://doi.org/10.5194/egusphere-2024-3945
Preprint. Discussion started: 15 January 2025

Regional sea level budget over 2004-2022

Marie Bouih[1], Anne Barnoud[1], Chunxue Yang[2], Andrea Storto[2],

Alejandro Blazquez[3] , William Llovel[4], Robin Fraudeau[1] and Anny Cazenave[3]

1. Magellium, 31520 Ramonville St Agne, France

2. Institute of Marine Science, National Research Council of Italy, Rome, Italy

3. Université de Toulouse, LEGOS (CNES/CNRS/IRD/UT3), 31401 Toulouse, Cedex, France

4. Univ Brest, CNRS, Ifremer, IRD, Laboratoire d'Océanographie Physique et Spatiale (LOPS), IUEM, F29280, Plouzané, France

Corresponding author : Anny Cazenave

anny.cazenave@univ-tlse3.fr; anny.cazenave@gmail.com

ORCID 0000-0002-2289-1858

https://doi.org/10.5194/egusphere-2024-3945
Preprint. Discussion started: 15 January 2025

ABSTRACT

Closure of the regional sea level budget is investigated over the 2004-2022 time span by comparing trend patterns from the satellite altimetry-based sea level with the sum of contributions, i.e. the thermosteric, halosteric, manometric and GRD (Gravitational, Rotational, and Deformational fingerprints due to past and ongoing land ice melt) components. The thermosteric and halosteric components are based on Argo data. For the manometric component, two approaches are considered: one using GRACE/GRACE-Follow On satellite gravimetry data, and the other using ocean reanalyses-based sterodynamic sea level data corrected for local steric effects. For the latter, six different ocean reanalyses are considered, including two reanalyses that do not assimilate satellite altimetry data. The results show significantly high residuals in the North Atlantic for both approaches. In other regions, small-scale residuals of smaller amplitude are observed and attributed to the finer resolution of altimetry data compared to the coarser resolution of data sets used for the components. Focus on the strong residual signal seen in the North Atlantic suggests Argo-based salinity errors in this region. However, it is not excluded that other factors also contribute to the non-closure of the budget in this region.

https://doi.org/10.5194/egusphere-2024-3945
Preprint. Discussion started: 15 January 2025

1. Introduction

On interannual to decadal time scales, sea level changes in a specific oceanic region arise from several factors. The global mean geocentric sea level rise is primarily driven by ocean warming, land ice melting, and water exchange with continents. Additionally, local and regional effects contribute, including changes in seawater density caused by variations in temperature and salinity (steric effects), as well as the redistribution of ocean water mass through circulation changes (manometric component, Gregory et al., 2019) and variations in atmospheric loading. Furthermore, changes in the solid Earth's gravity, rotation, and deformation (GRD) occur in response to mass redistributions from past and present-day land ice melt and land water storage changes. These GRD factors include two components : the Glacial Isostatic Adjustment (GIA) effect, which stems from the last deglaciation, and GRD fingerprints, which are associated with contemporary land ice melting and, to a lesser extent, changes in land water storage (Gregory et al., 2019).

In terms of global average, the rate of sea level rise is dominated by ocean warming via thermal expansion of seawater, and land ice melting (from glaciers, Greenland and Antarctica ice sheets), in response to global warming (e.g., Cazenave et al., 2018, Nerem et al., 2018, Cazenave and Moreira, 2022, IPCC, 2019, 2021; Llovel et al., 2023). The spatial variations of the rate of sea level rise mainly result from steric effects, with the thermosteric contribution being generally dominant (e.g., Stammer et al., 2013, Hamlington et al., 2020), except in the Arctic where the halosteric effect is important (e.g., Carret et al., 2017; Tajouri et al., 2024).

Many studies have computed the global mean sea level budget over the altimetry era (i.e., since the early 1990s) by comparing the global mean sea level rise with the sum of the thermal and mass components from independent observing systems (e.g., Dieng et al., 2017, Nerem et al., 2018, WCRP, 2018, Horwath et al., 2022, Chen et al., 2018, 2020, Barnoud et al., 2021, 2023, to focus only on the most recent publications). These studies have shown that at least until 2016, the global mean sea level budget is closed within the data uncertainties. In recent years, some discrepancy has been observed between the altimetry-based global mean sea level and the sum of the Argo-based steric and gravimetry-based mass components (e.g., Chen et al., 2020, Barnoud et al., 2023, Mu et al., 2024), especially when using the Gravity Recovery And Climate Experiment (GRACE) and GRACE Follow-On (GRACE-FO) satellite data to estimate the manometric sea level change, instead of individual mass contributions (i.e., glaciers, Greenland and Antarctica ice sheets, land waters and atmosphere water vapour). At regional scale, the closure of the sea level budget has been less studied so far. A

https://doi.org/10.5194/egusphere-2024-3945
Preprint. Discussion started: 15 January 2025

few recent studies have assessed the closure of the sea level budget at the basin-scale, over the altimetry era (e.g., Rietbrock et al., 2016, Frederiske et al., 2016, 2018, 2020; Hamlington et al., 2020, Royston et al., 2020, Camargo et al., 2023, Mu et al., 2024). The regional ocean mass budget has also been investigated (Ludwigsen et al., 2024). Closure of the regional budget is only observed in some regions but not everywhere. For example, using altimetry, gravimetry and Argo data over 2005-2015, Royston et al. (2020) concluded that the regional budget cannot be closed in the Indian-South Pacific region. Similarly, Camargo et al. (2023) also found non-closure of the regional sea level budget in a number of oceanic areas. Using machine learning techniques, these authors were able to identify processes not well captured by the observations that are considered to assess closure of the regional sea level budget.

In the above studies, closure of the regional budget was assessed by averaging the data either at basin-scales or sub-basin scales. In the present study, we revisit the regional sea level budget over the GRACE/Argo era (starting in 2004) at the local scale, without averaging the data at the basin-scale. After removing the global mean trend of each component, we focus on the spatial trend patterns, with a resolution of about 300 km, as allowed by the gridded data sets considered, an approach not applied in the previous studies. This approach avoids compensation of spurious positive/negative sub-basin trend patterns and allows for more precise identification of the areas where the sea level budget is not closed.

For this investigation, we used gridded satellite altimetry data for the observed sea level changes and Argo data to estimate the thermosteric and halosteric sea level changes. For the manometric component, two types of data are considered: satellite gravimetry data from the GRACE and GRACE FO missions as well as ocean reanalyses to estimate the redistribution of water mass already in the ocean (following the same approach as in Camargo et al., 2023, i.e., estimating sterodynamic sea level changes corrected for local steric effects; see section 3). The study period covers the period from January 2004 to December 2022 (although some data sets end in December 2019; section 3).

https://doi.org/10.5194/egusphere-2024-3945
Preprint. Discussion started: 15 January 2025

2. Brief overview of the sea level components at regional scale

2.1. Steric component

The steric component includes the effects of ocean temperature and salinity changes. Remote surface wind forcing, heat and freshwater fluxes associated with variations in the overlying atmospheric state are the two main forcing mechanisms causing steric changes (Stammer et al., 2013, Roberts et al., 2016). Wind forcing modifies the ocean circulation which further redistributes heat and water masses. It is the dominant mechanism of interannual to decadal steric changes in many regions, particularly in the tropics (e.g., Timmermann et al., 2010; Merrifield and Maltrud, 2011; Piecuch and Ponte, 2014; England et al., 2014). Wind forcing can also play a role in the extra tropics and at high latitudes (Roberts et al., 2016). Buoyancy forcing, i.e. surface air-sea fluxes of heat and freshwater (due to surface warming and cooling of the ocean, and exchange of freshwater with the atmosphere and land through evaporation, precipitation, and runoff) is important in mid to high latitudes, e.g., in the North Atlantic Ocean (Gulf Stream and North Atlantic subpolar gyre) (Roberts et al., 2016).

Over the altimetry era, regional sea level patterns are dominated by steric changes. In most regions, the thermosteric component by far dominates the halosteric one, except in the North Atlantic Ocean (Llovel and Lee, 2015) and in high latitude areas, e.g., in the northeast Pacific, and particularly in the Arctic (e.g., Carret et al., 2016; Ludwigsen et al., 2022, Tajouri et al., 2024). On interannual to multidecadal time scales, the spatial trend patterns in (thermo) steric sea level are still largely influenced by basin-scale internal climate modes of variability, e.g., El Niño-Southern Oscillation (ENSO), Pacific Decadal Oscillation (PDO), Atlantic Multidecadal Oscillation (AMO), North Atlantic Oscillation (NAO) and Indian Ocean Dipole (IOD). Wind stress changes on such time scales are indeed directly related to climate modes (Han et al., 2017). For example, sea level in the tropical Pacific oscillates from west to east with ENSO (with high/low sea level in the eastern/western part during El Niño/La Niña events), in response to wind-forced propagating waves. In the North Atlantic, surface wind and heat flux partly drive interannual to decadal sea level fluctuations and are associated with the NAO (but changes in the Atlantic Meridional Ocean Circulation also contribute) (Han et al., 2017). In the tropical Indian Ocean, interannual to decadal variability in sea level is strongly influenced by ENSO and the IOD (Han et al., 2017, 2019).

https://doi.org/10.5194/egusphere-2024-3945
Preprint. Discussion started: 15 January 2025

2.2. Manometric component

The regional manometric sea level change essentially results from spatial redistribution of water mass already in the ocean by the ocean circulation, plus the total water mass added to the ocean (the latter being called barystatic component; Gregory et al., 2019), due to land ice melt and to the exchange of water with the continents. The barystatic contribution nearly uniformly covers the oceanic domain rapidly (within a few weeks) via a barotropic global adjustment occurring on short time scales (Lorbacher et al., 2012). Because the global mean trend of each component of the regional sea level budget is removed in this study, the barystatic component disappears. Compared to steric changes, the manometric sea level change due to water mass redistribution (barystatic contribution removed), plays a smaller role on interannual to decadal time scales, but can be sizeable (e.g., Dangendorf et al., 2021, Wang et al., 2022), in particular at high latitudes and over shallow continental shelves (e.g., Forget and Ponte, 2015; Carret et al., 2021).

2.3. Atmospheric loading

On seasonal and longer time scales, sea level responds as an inverted barometer to atmospheric loading (Wunsch and Stammer, 1997) i.e. the sea surface height increases (decreases) by 1 cm if the local surface pressure decreases (increases) by approximately 1 mbar. The atmospheric loading component is quite small compared to the thermosteric one, but it is non-negligible at high latitudes (e.g., in the Arctic Ocean where it can reach 0.3 mm/yr on interannual to decadal time scales, Proshutinski, 2004). Atmospheric loading can be estimated using e.g. surface pressure data from atmospheric reanalyses. Note that it does not affect the global mean sea level because of mass conservation.

2.4. Gravity, Earth Rotation, and solid Earth Deformations (GRD)

The response of the solid Earth to past and present-day water mass exchange between continents and oceans causes global and regional sea level changes. The GIA results from the ice and water mass redistribution of the last deglaciation. Its effect depends on the Earth's mantle viscosity and deglaciation history. The response of the solid Earth to ongoing land ice melt essentially depends on the elasticity of the lithosphere and mantle, as well as on the amount and location of ice mass loss. These mass redistributions induce changes in the gravity, rotation, and visco-elastic deformations of the solid Earth (Mitrovica et al., 2001; Milne et al., 2009; Stammer et al., 2013). These are the so-called GRD (Gravity, Earth Rotation, and solid Earth Deformations) fingerprints (Gregory et al., 2019). In the literature, the GRDs are

https://doi.org/10.5194/egusphere-2024-3945
Preprint. Discussion started: 15 January 2025

often separated into the ones resulting from the GIA (last deglaciation) and the contemporary GRDs, the latter referring to mass redistributions due to present-day land ice melt and land water storage variations. In terms of global average, the GIA effect on sea level change is around -0.3 mm/yr (Peltier, 2004; Tamisiea, 2011;, Caron et al., 2018). Its regional signature is mostly uniform, except in formerly glaciated high-latitude regions. The contemporary GRD fingerprints produce complex regional patterns in sea level change : sea level drops near the melting bodies but sea level rises in the far field (e.g., along the northeast coast of America). Several studies have theoretically computed the impact of contemporary GRD changes on relative and absolute sea levels, by solving the sea level equation, either assuming a priori current ice sheet mass loss (e.g., Mitrovica et al., 2001, Tamisiea, 2011, Spada, 2017), or using realistic ice mass loss based observations from the GRACE satellite gravimetry mission (Adhikari et al., 2019). Note that the sea level fingerprints associated with the GIA and the contemporary GRDs are mostly expressed in terms of linear trends and have a small amplitude compared to the observed regional sea level and steric sea level trends. However, with the expected increase of land ice melt in the coming decades, the contribution of the contemporary GRD fingerprints to regional sea level trends may become increasingly significant.

3. Data and methods

3.1. Data

3.1.1 Total sea level

The total sea level is routinely observed by satellite altimetry. In this study, we use the daily 1/4° x 1/4° gridded sea level anomaly data from the Copernicus Climate Change Service (C3S) Climate Data Store (CDS) (Copernicus Climate Change Service, 2018). To ensure the long-term stability of this altimetry-based data, C3S sea level anomalies rely on two simultaneous satellite missions at any given time : the successive reference missions (TOPEX/Poseidon, Jason-1, Jason-2, Jason-3, and Sentinel-6 Michael Freilich) plus an auxiliary mission from the global constellation. The dataset is corrected for TOPEX-A altimeter drift (Ablain et al., 2017), as well as for the Jason-3 radiometer drift that impacts the wet troposphere correction (Brown et al. 2023). The dataset covers the period from January 1993 to December 2023. The C3S dataset is corrected for GIA using the ICE6G-D model (Peltier et al., 2018). Total sea level uncertainties are derived following Ablain et al. (2019) and updated by Guérou et al. (2023).

https://doi.org/10.5194/egusphere-2024-3945
Preprint. Discussion started: 15 January 2025

3.1.2 Steric sea level

We use the Argo-based steric sea level data from the Scripps Institution of Oceanography (SIO), which provides monthly gridded data at a 1° x 1° resolution (Roemmich and Gilson, 2009). The choice for the SIO product is motivated by the fact that its post-processing corrects for the salinity drift reported in Argo floats since 2015, which misleads to a spurious increase reported in the global mean salinity (Wong et al., 2023; Liu et al., 2020, 2024; Ponte et al., 2021). This salinity drift has a significant impact on the sea level budget closure (Chen et al., 2020; Barnoud et al., 2021). The SIO processing methodology considers the most up-to-date delayed-mode Argo profiles which have been meticulously quality-controlled by a scientist (typically within 1-2 years after the float transmits the data). In addition, the SIO processing adjusts the real-time Argo profiles (which have passed through automatic quality-control typically within 24 h) to fit the WOCE (World Ocean Circulation Experiment) global hydrographic climatology. This specific processing has the benefit of removing the salinity drift in the SIO steric sea level data (Liu et al., 2024). The dataset covers the period from January 2004 to December 2022, within the 0–2000 m depth range, and the latitudes between 66°S and 66°N.

In this study, the deep ocean's contribution to steric sea level is not considered due to its small magnitude and possibly high uncertainty (e.g., Purkey and Johnson, 2010). The thermosteric steric sea level, halosteric sea level and total steric sea level changes are computed from the temperature and salinity gridded data using the lenapy library (https://github.com/CNES/lenapy) from the Centre National d'Études Spatiales (CNES), based on the Gibbs seawater oceanography toolbox of the 2010 Thermodynamic Equation Of Seawater (TEOS-10).

3.1.3 Manometric sea level

The manometric sea level change is estimated using two independent methods.

The first approach relies on satellite gravimetry data from the GRACE mission (2002-2017, Tapley et al., 2019) and GRACE-FO mission (launched in 2018, Landerer et al., 2020), which enables to estimate changes in the Earth's gravitational field linked to mass redistribution, including the regional sea level variations due to GRD effects. Two sources of GRACE solutions are considered:

- (1) An ensemble mean of so-called mass concentration (mascon) solutions. We use the latest GRACE and GRACE-FO Release 6 mascon solutions from the Center for Space Research (CSR; Save et al., 2016), Jet Propulsion Laboratory (JPL; Watkins et al., 2015), and Goddard Space Flight Center (GSFC; Loomis et al., 2019). These mascon solutions are corrected for the GIA effect using the ICE6G-D model (Peltier et

https://doi.org/10.5194/egusphere-2024-3945
Preprint. Discussion started: 15 January 2025

al., 2018), as well as for the geocenter motion using the correction from Sun et al. (2016). The manometric component is estimated as the mean of these three gridded ocean mass products, which are given in equivalent water height.

- (2) An ensemble of 60 spherical harmonic solutions. This ensemble is derived from the manometric GRACE-based products (DOI: 10.24400/527896/a01-2023.011 version 4.0) and distributed at AVISO+ (https://aviso.altimetry.fr) . This product allows for uncertainty estimates linked to various stages of GRACE and GRACE-FO data processing (Blazquez et al, 2018). This ensemble of 60 solutions results from the combination of five processing centres, three C20/C30 (spherical harmonics of degree 2 and 3 of the gravity field potential) estimates, two GIA models (ICE6G-D from Peltier et al., 2018 and the model from Caron et al., 2018), and two filtering levels. The geocenter motion is corrected with a model based on the approach developed by Sun et al. (2016) and Swenson et al. (2008). Each ensemble member is also corrected for the water vapor mass in the atmosphere using the C0 from GAA (Chen et al, 2019). For each ensemble member, atmospheric loading over the ocean is restored using the GAD products (Flechtner et al., 2015) to correct for the inverse barometer effect, aligning the ocean mass variations with satellite altimetry data in which atmospheric loading is already accounted for.

The two sets of GRACE data used here cover the period from January 2004 to December 2022.

The second approach follows Camargo et al. (2023) method which derives the manometric sea level change from ocean reanalyses. Ocean models provide the sterodynamic sea level change, i.e., the sea level change due to changes in ocean density and circulation, with the inverse barometer correction applied (Gregory et al., 2019; Storto et al., 2024). The corresponding manometric component is derived by correcting the reanalysis-based sterodynamic sea level by the local steric effect and adding the contemporary GRD fingerprints. It is the approach followed here. Due to the temporal availability of some reanalyses, part of the analyses only cover the period from January 2004 to December 2019, while others are extended to December 2022.

We consider six different ocean reanalyses with different characteristics as listed in Table 1. GLORYS, C-GLORS, ORAS5, and FOAM use the NEMO (Nucleus for European Modelling of the Ocean) ocean model and assimilate satellite altimetry-based sea level data. The SODA reanalysis is based on the MOM (Modular Ocean Model) developed by NOAA (National Oceanographic and Atmospheric Administration, USA) and does not include altimetry data. All these reanalyses have a spatial resolution of 0.25°. In order to assess the regional sea level budget with another manometric component independent of satellite altimetry data, we also consider an ensemble reanalysis at lower resolution and without altimetry data

https://doi.org/10.5194/egusphere-2024-3945
Preprint. Discussion started: 15 January 2025

assimilation (called CIGAR; see Table 1). This variety of reanalyses offers the opportunity to evaluate the degree of consistency of the manometric signal from reanalysis-based products.

Table 1 : Characteristics of the six ocean reanalyses used in this study to estimate the manometric sea level change patterns independently from GRACE and GRACE-FO data.

Reanalysis	Ocean model, Spatial Resolution, End date	Data assimilation of altimetry-based sea level data	References
GLORYS (MOI)	NEMO, 0.25°, 2022	Yes	Garric and Parrent (2017)
C-GLORS (CMCC)	NEMO, 0.25°, 2022	Yes	Storto and Masina (2016)
ORAS5 (ECMWF)	NEMO, 0.25°, 2022	Yes	Zuo et al. (2019)
FOAM (UK Metoffice)	NEMO, 0.25°, 2022	Yes	Blockley et al. (2014)
SODA (Version 3.4.2, U.Maryland)	MOM4, 0.25°, 2019	No	Carton et al. (2018)
CIGAR (CNR-ISMAR)	NEMO, 1°, 2022	No	Storto and Yang (2024)

To compare the manometric component derived from ocean reanalyses with the one based on GRACE and GRACE-FO, we added the contemporary GRD contribution to the reanalysis-based manometric sea level change. We used the sea level fingerprint data from Adhikari et al. (2019), which provides monthly contemporary GRD fingerprints at a 0.5° x 0.5° resolution. Because the Adhikari et al. (2019) data set ends in 2016, we linearly extrapolated the GRD fingerprints up to 2022 and added the corresponding trends to the ocean reanalyses-based manometric trends.

https://doi.org/10.5194/egusphere-2024-3945
Preprint. Discussion started: 15 January 2025

3.2. Method

Systematic corrections for both atmospheric loading and GIA effects are applied to altimetry-based and satellite gravimetry datasets, even though different models are used in each dataset. The MOG2D (Carrere and Lyard, 2003) and inverse barometer model is used for altimetry data (www.aviso.altimetry.fr), while the GAD product, which represents monthly mean ocean bottom pressure due to non-tidal dynamic oceanic and atmospheric mass variations, is used for GRACE and GRACE-FO data. It is based on the AOD1B model (Flechtner et al., 2015). Likewise, the GIA corrections rely on the ICE6-G model for altimetry (Peltier et al. 2018), while GRACE datasets use either ICE6-G (Peltier et al. 2018) or Caron et al. (2018) models.

All datasets were spatially interpolated onto a 1° x 1° grid and were averaged on a monthly basis. For spatial consistency, a common masking technique was applied to all gridded components. This mask covers latitudes from 66°S to 66°N, excludes inland seas, and omits coastal regions where the distance from land is less than 300 km. A spatial 3° x 3° Lanczos filter was then applied to each grid to smooth out the highest resolution features not observed by all observing systems.

Finally, seasonal signals (annual and semi-annual) were removed at each grid mesh of each data set through a simple least-squares adjustment of 6-month and 12-month sinusoids, and a 3-month Lanczos filter was applied locally to each dataset to remove high frequency signals. The global mean trend of each dataset computed over the study period was also removed.

All datasets span from January 2004 to December 2022, except for the oceanic reanalyses-based manometric components for which two study periods were considered, depending on the dataset availability: January 2004-December 2019 and January 2004-December 2022.

4. Results : Regional sea level budget with GRACE and Argo

4.1. Trend patterns in observed sea level, components and residuals

Figure 1 shows the maps of altimetry-based sea level trends, of the GRACE- and Argo-based component trends, and of the residual trends (i.e., trend differences between altimetry-based sea level and sum of components).

https://doi.org/10.5194/egusphere-2024-3945
Preprint. Discussion started: 15 January 2025

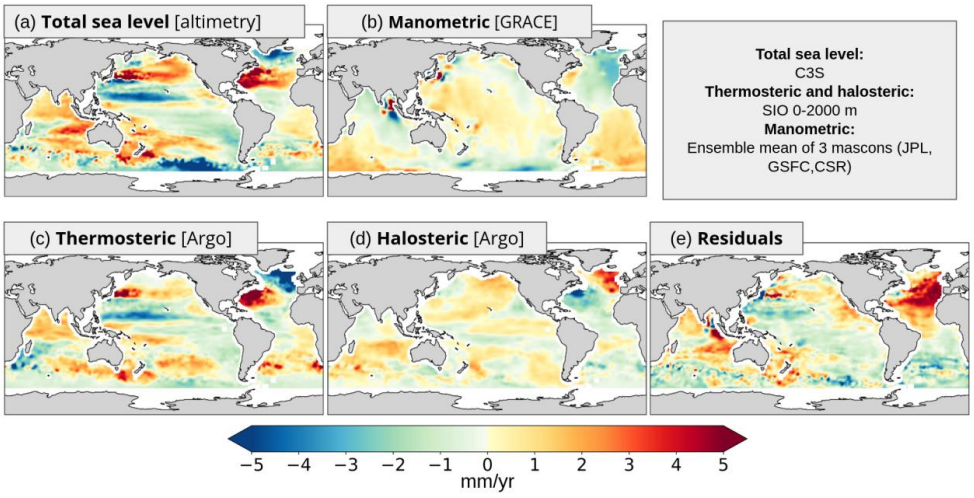

Figure 1: Sea level trends over January 2004 to December 2022 in observed altimetry-based sea level (a), components (b, c, d: GRACE-based manometric, Argo-based thermosteric and Argo-based halosteric sea level) and budget residual trends (observed sea level minus sum of components) (e).

Visual inspection of Figure 1 confirms earlier findings, i.e., the observed regional trend patterns are dominated by the thermosteric trend patterns (e.g., Stammer et al., 2013; Hamlington et al., 2020; Cazenave and Moreira, 2022). The manometric and halosteric components have in general lower amplitude than the thermosteric one, except in the North Atlantic where thermosteric and halosteric trends have opposite signs (e.g., Stammer et al., 2013).

The residual map shows that in many regions, the sum of components does not cancel out the observed trends. This is the case in the North Atlantic where a strong positive residual is observed. In this region, altimetry-based sea level displays positive trends in the western part and negative trends south of Greenland. The opposite patterns in the thermosteric and halosteric components of the North Atlantic agree well in terms of regional extent but a larger amplitude is noted in the thermosteric component. It is worth noting that the North Atlantic manometric sea level has similar patterns as the thermosteric ones but they are more diffuse (possibly due to the lower resolution of GRACE data) and of lower amplitude.

In the northeast Atlantic, the observed strong residuals result from an absence of signal in this region in the thermosteric and halosteric component combined with a slightly negative signal in the manometric component, possibly a result of errors in both GRACE and Argo datasets. The strong residual signal in the North Atlantic is discussed in detail in section 6.

https://doi.org/10.5194/egusphere-2024-3945
Preprint. Discussion started: 15 January 2025

Another striking observation from Figure 1 is that large-scale residuals over the Pacific, Indian, North and South Atlantic Oceans are anti-correlated to those of the manometric sea level. This is highlighted in Figure 2. A priori, such an anti-correlation would suggest that the large-scale residual patterns are caused by spurious GRACE signal since its removal in the altimetry-based sea level trends corrected for the Argo-based steric component does not lead to cancellation.

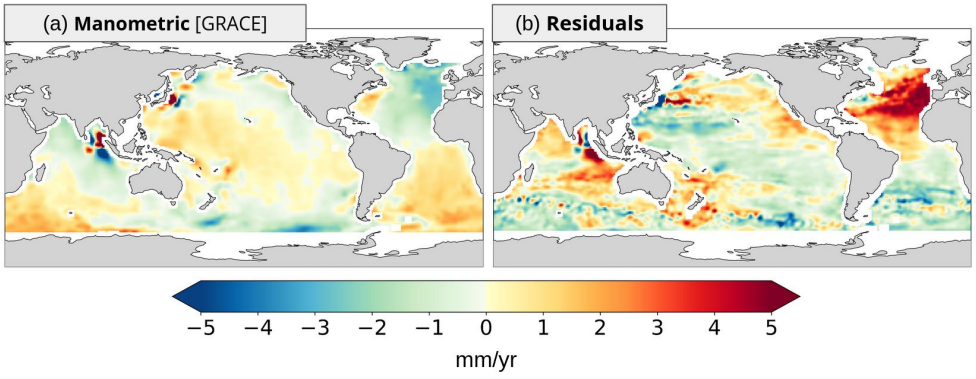

Figure 2: Large-scale trend patterns in the GRACE-based manometric sea level (a) and residuals (b).

4.2. GRACE data assessment

To explore the origin of the observed large-scale anti-correlation between GRACE-based manometric and residual trends, we analysed the effects of the geocenter and GIA corrections applied to GRACE data. To assess the contribution of low degrees to the sea level budget residuals, we decomposed the sea level budget components into spherical harmonics and computed the residuals for various configurations of low degree harmonics (see supplementary information, SI). Figure S1 and Table S1 show that degree 1,0 (related to the geocenter motion) and degree 2,1 (related to polar motion and GIA correction) harmonics contribute to the high residuals in the North Atlantic Ocean.

GRACE data are classically corrected for the geocenter motion when compared with altimetry data, which leads to moving GRACE observations from the centre of mass to the centre of figure of the reference system. However, the theoretical basis for correcting GRACE data for the geocenter motion when comparing with altimetry remains unclear. Indeed, altimetry data

https://doi.org/10.5194/egusphere-2024-3945
Preprint. Discussion started: 15 January 2025

are supposed to be also provided in a centre of mass reference system, the satellite orbits being expressed in such a reference system (Alexandre Couhert, personal communication).

Using the ensemble of 60 spherical harmonic solutions described in Section 3.1, we constructed an alternative ensemble of 60 solutions without applying the correction for the geocenter motion, i.e. keeping the GRACE observations in the centre of mass reference system. Comparing these two ensembles of solutions allows us to assess the influence of the geocenter correction on the manometric component and, consequently, on the residuals of the sea level budget. Figure 3 shows the impact of the geocenter correction on the manometric trends as well as on the associated residual trends. Not correcting for the geocenter motion reduces the residuals observed in the North Atlantic Ocean but increases the residual trends elsewhere, with larger residuals in almost all other ocean basins. Thus, even if the Sun et al. (2016)'s geocenter correction may not be optimal, it minimizes the residual trends everywhere, except in the northeast Atlantic Ocean. This questions the actual referential of altimetry data and the consistency of the processing between satellite altimetry and satellite gravimetry data. Besides, if no geocenter correction should be applied, this means that GRACE observes large scale signals not observed by altimetry data, so that one may wonder whether some altimetry data corrections and post-processing could alter large-scale signals.

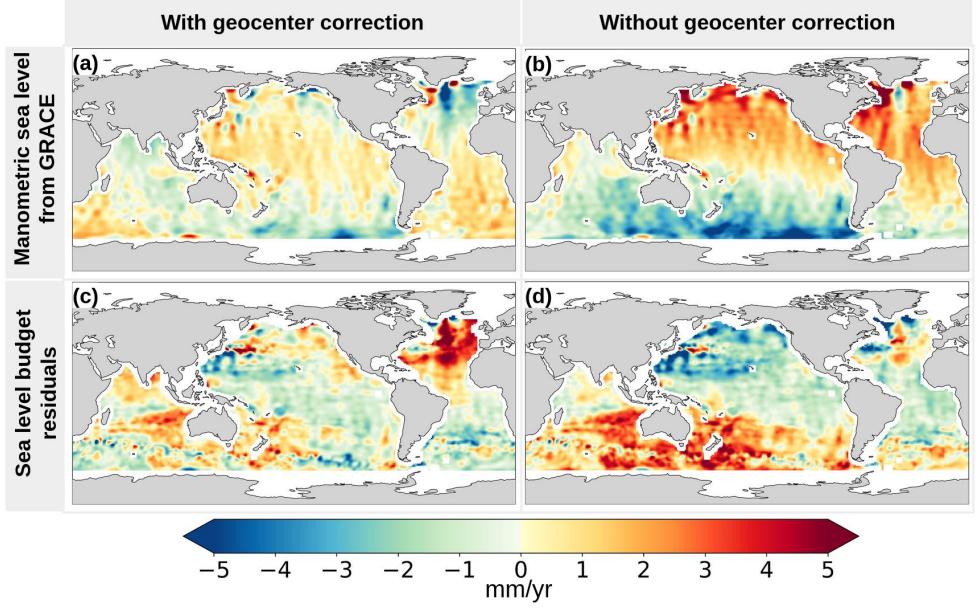

Figure 3: Sea level trends of manometric and corresponding budget residuals with and without geocenter correction. (a) Manometric sea level trend map with the geocenter correction, (b) Manometric sea level trend map without the geocenter correction, (c) Sea level budget

https://doi.org/10.5194/egusphere-2024-3945
Preprint. Discussion started: 15 January 2025

residual trend map computed with the manometric component corrected for the geocenter, (d) Sea level budget residual trend map computed with the manometric component not corrected for the geocenter.

To estimate the impact of the GIA corrections on the manometric component and budget residuals, we further formed two separate subsets of 30 solutions each for each GIA model (Peltier et al, 2018 and Caron et al., 2018), applying the Sun et al. (2016)'s geocenter correction to each subset. Unlike for the geocenter case, no significant difference was observed.

5. Regional sea level budget using ocean reanalyses for the manometric component

As explained in section 2, according to Gregory et al. (2019) and Camargo et al. (2023), the dynamic ocean mass redistribution due to ocean circulation changes can be estimated from the sterodynamic sea level corrected for local steric changes. Thus, in this study, we apply here the Camargo et al. (2023)'s approach and use ocean reanalyses to estimate the manometric component, in order to further assess closure of the regional sea level budget.

As detailed above (section 3), six different ocean reanalyses have been considered over their common period from January 2004 to December 2019. Figure 4 shows the reanalysis-based manometric trend maps over 2004-2019, for each of the six data sets, as well as their mean. The manometric components based on the two sets of GRACE solutions, restricted to this study period, are also shown.

https://doi.org/10.5194/egusphere-2024-3945
Preprint. Discussion started: 15 January 2025

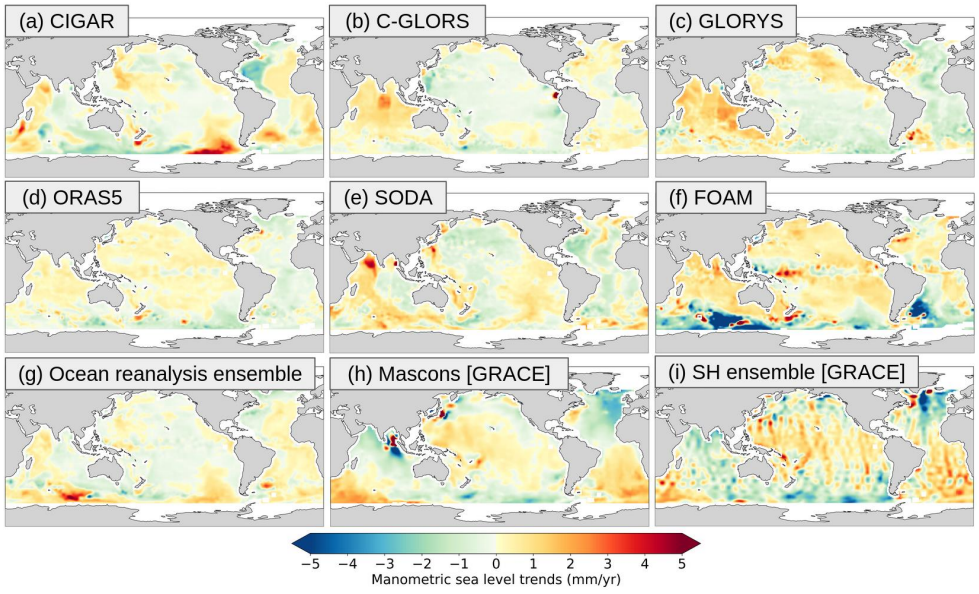

406

407 *Figure 4: Reanalysis-based manometric trend maps over January 2004-December 2019 for*
408 *each of the six ocean reanalyses: CIGAR, C-GLORS, GLORYS, ORAS5, SODA and FOAM*
409 *(panels a to f). Panel (g) shows the ensemble mean of the six reanalyses. Panels h and i refer*
410 *to the manometric component from the GRACE mascon and GRACE spherical harmonic (SH)*
411 *ensembles.*
412

413 The six reanalyses provide quite different manometric trend patterns. The FOAM and ORAS5
414 patterns are quite similar in the Pacific and Indian Oceans. In these regions, C-GLORS,
415 CIGAR and GLORYS show rough agreement. SODA's patterns differ from the other
416 reanalyses everywhere, although they look similar to CIGAR in the Indian Ocean.

417 Two statements can be made by comparing reanalyses-based averaged map with the
418 GRACE-based manometric map : (1) the spatial patterns of the reanalysis-based manometric
419 trend map have generally lower amplitude than the GRACE ones, and (2) except in the North
420 Atlantic, the spatial trends of the ensemble mean reanalyses and GRACE have opposite signs.

421 The regional budget has been computed with each of the six reanalyses as well as their mean,
422 all other data being kept unchanged. The corresponding residual trend patterns are shown in
423 Figure 5.

https://doi.org/10.5194/egusphere-2024-3945
Preprint. Discussion started: 15 January 2025

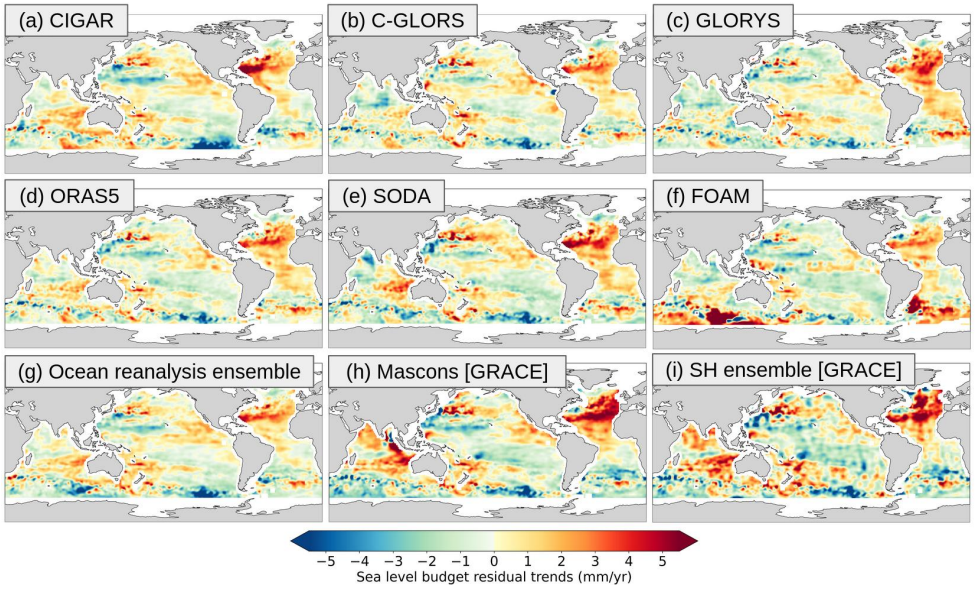

Figure 5: Residual trends of the regional sea level budget computed with each of the six reanalyses-based manometric data sets, as well as with their mean (panels a to g) (with altimetry-based and steric components unchanged). GRACE-based residual trends for both mascons and spherical harmonic solutions are also shown (panels h and i). The period of analysis here is from January 2004 to December 2019.

The CIGAR, C-GLORS, SODA, ORAS5, and GLORYS reanalyses give very similar residual trend patterns, even though SODA uses completely different ocean models, data assimilation schemes, and no altimetry-based sea level anomaly data assimilated. Note that CIGAR does not either assimilate altimetry-based sea level anomaly data, but it is forced by the latest atmospheric reanalysis from ECMWF (unlike the other reanalyses) and embeds a daily varying runoff dataset for freshwater discharge into the oceans. One outlier is FOAM which shows strong positive residual trends in the southern Atlantic and Indian Oceans. The ensemble mean residual trend map displays a lower signal than the GRACE cases (panels h and i of Figure 5). What is striking is that the two approaches (reanalyses and GRACE) show positive residual trends in the North Atlantic. However, the residuals are significantly stronger using GRACE, especially in the northeastern part of the Atlantic Ocean. This will be discussed in section 6.

Table 2 shows the root mean square (RMS) of the gridded residuals trends over 2004-2019, averaged over the Pacific, Indian, North and South Atlantic Oceans for the reanalyses and GRACE cases.

https://doi.org/10.5194/egusphere-2024-3945
Preprint. Discussion started: 15 January 2025

If we except FOAM which displays higher RMS in the Indian and South Atlantic Oceans than other reanalyses, Table 2 clearly shows systematically higher RMS (in the range 2-3 mm/yr) in the North Atlantic Ocean for the C-GLORS, SODA, GLORYS and ORAS5 reanalyses as well as for GRACE mascons.

Table 2: RMS of gridded residuals trends over 2004-2019, averaged over the Pacific, Indian, North and South Atlantic Oceans for the GRACE and reanalyses cases.

RMS (mm/yr)	Pacific	Indian	North Atlantic	South Atlantic
C-GLORS	1.48	1.46	2.02	1.35
FOAM	1.66	2.81	1.99	2.54
SODA	1.58	1.79	2.68	1.56
GLORYS	1.34	1.61	2.49	1.72
ORAS5	1.39	1.38	2.15	1.37
GRACE mascons	1.51	1.78	2.92	1.43

Because four of the reanalyses used above assimilate altimetry data (i.e., C-GLORS, GLORYS, ORAS5 and FOAM), our approach may introduce some circularity to the regional sea level budget assessment. This is the reason for also using reanalyses without altimetry data assimilation (SODA and CIGAR). Here we focus on CIGAR and extend the study period to December 2022. Results are shown in Figure 6. Comparing the manometric components of two versions with and without altimetry data assimilation (e.g., C-GLORS and CIGAR, noting however that they differ in terms of resolution, configuration and forcing) shows some differences locally, in particular in the northwestern Atlantic and North Indian Oceans. However, the residual trend maps are very similar. The case without altimetry data assimilation (CIGAR) still shows significant residual signal in the North Atlantic Ocean. This observation points to the steric component (and possibly the halosteric component) as the main suspect for the non-closure of the budget in the North Atlantic Ocean.

https://doi.org/10.5194/egusphere-2024-3945
Preprint. Discussion started: 15 January 2025

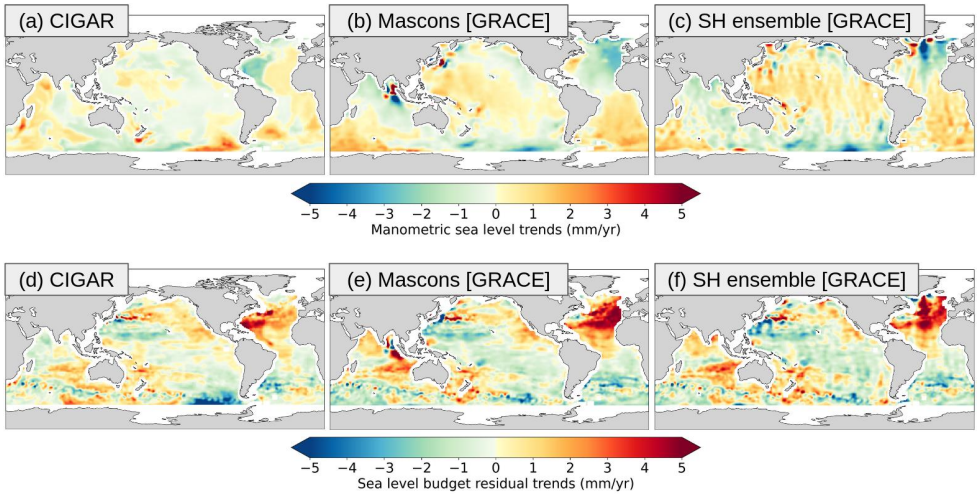

Figure 6: Manometric component based on the CIGAR reanalysis (reanalysis without altimetry data assimilation) (panel a), and the two GRACE solutions (panels b and c). Sea level budget residuals using the CIGAR-based manometric component (panel d) and the two GRACE manometric components (panels e and f). The period of analysis here is from January 2004 to December 2022.

6. Residual trends in the North Atlantic Ocean

In this section, we focus on the North Atlantic Ocean where positive residuals are observed when using either GRACE or the CIGAR reanalysis for estimating the manometric component.

Figure 7 shows each component of the budget over the North Atlantic Ocean over January 2004-December 2022, computed using three manometric component estimates: GRACE mascons, ensemble mean GRACE SH and CIGAR reanalysis. Associated residual maps (all components unchanged except the manometric one) are also shown.

https://doi.org/10.5194/egusphere-2024-3945
Preprint. Discussion started: 15 January 2025

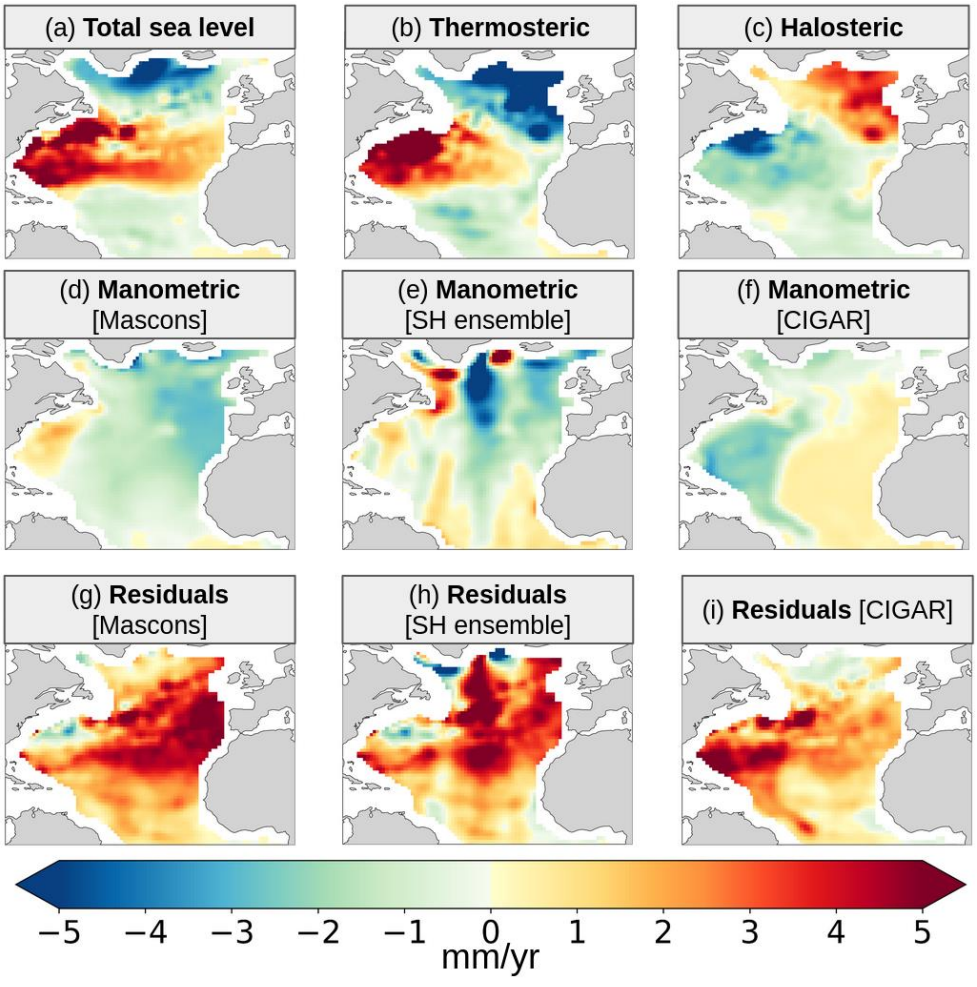

Figure 7: North Atlantic Ocean sea level trends (mm/yr) over January 2004 to December 2022: Observed altimetry-based sea level (a), Argo-based thermosteric and halosteric components (b,c), manometric components from GRACE mascon (d), ensemble mean GRACE spherical harmonics (e) and derived from CIGAR reanalysis (f). Sea level budget residuals (observed sea level trends minus sum of component trends) using GRACE mascon (g), ensemble mean GRACE spherical harmonics (h) and CIGAR (i).

The North Atlantic Ocean residuals of all three manometric component cases (GRACE mascons, ensemble mean GRACE spherical harmonics and CIGAR) show a positive signal. However, the patterns are significantly different between the reanalysis and GRACE cases. They are localized in the western part of the tropical North Atlantic Ocean with the CIGAR reanalysis and in the eastern part (between the Gibraltar Strait and the Gascogne Gulf) with GRACE mascons. The residuals based on the ensemble mean GRACE spherical harmonics display a strong north-south signal in the mid North Atlantic, likely due to north-south strip

https://doi.org/10.5194/egusphere-2024-3945
Preprint. Discussion started: 15 January 2025

noise affecting spherical harmonic solutions (Blazquez et al., 2018). CIGAR differentiates the sign of the patterns from the mid-Atlantic ridge, likely due to its effect on the basin-scale barotropic circulation. This effect is not seen in the gravimetry-based trends. To further investigate the North Atlantic sea level misclosure, we computed the North Atlantic sea level budget after geographically averaging each component over the region, using GRACE mascons for the manometric component. This is shown in Figure 8, along with the sea level budget, averaging the data globally but excluding the North Atlantic Ocean.

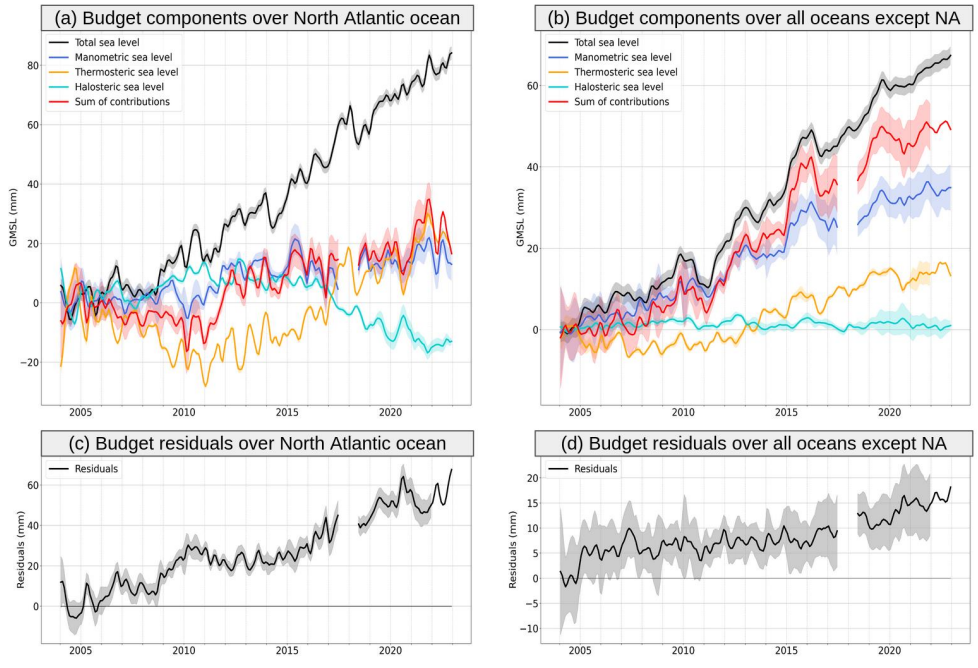

Figure 8: Regionally averaged sea level budget for January 2004 to December 2022, over the North Atlantic Ocean (a) and over all oceans except the North Atlantic (NA) one (b). On each panel are shown the altimetry-based sea level (black curve), the thermosteric and halosteric components (orange and turquoise curves), the manometric component (GRACE mascons, blue curve) and the sum of all components (red curve). The panels c and d show the corresponding residuals (observed sea level minus sum of components). Shaded areas represent the standard one-sigma uncertainties.

Figure 8 well confirms the non-closure of the budget over the North Atlantic Ocean, with a significant positive residual trend, whereas in the remaining oceanic domain, no significant residual trend is noticed. Figure 8 (panel a) suggests that the North Atlantic residual trend is related to the observed decrease of the halosteric component as of 2013-2014. A similar finding is provided in Mu et al. (2024).

https://doi.org/10.5194/egusphere-2024-3945
Preprint. Discussion started: 15 January 2025

We performed an Empirical Orthogonal Decomposition (EOF) of the gridded halosteric time series over 2004-2022 (global mean trend removed). The dominant mode (mode 1) is shown in Figure 9. The mode 1 principal component (PC) has a strange temporal behavior, with a significant slope as of 2013 (right panel), likely associated with the strong signal seen in the North Atlantic Ocean on the spatial map (left panel).

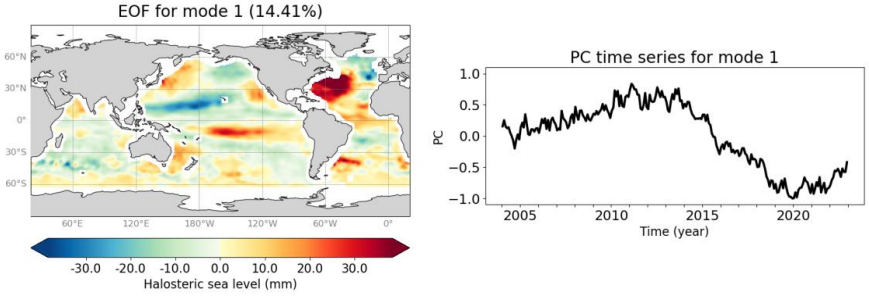

Figure 9: Mode 1 of the EOF decomposition of the gridded halosteric component over 2004-2022. Spatial map (left panel). Principal component (right panel). This first mode accounts for 14.4 % of the total halosteric signal.

7. Conclusion

In this study, we have revisited the regional sea level budget over the GRACE and Argo era. Using different data sets for the manometric component (GRACE and ocean reanalyses), we found significant non-closure of the budget in the North Atlantic Ocean in all studied cases. However, the residual patterns are not localized over the same areas in the GRACE and ocean reanalyses cases. They are stronger in the northeast Atlantic Ocean when considering the GRACE manometric component (mascon solution) while they are more localized in the western tropical part with the reanalysis-based manometric component. The sea level budget averaged over the whole North Atlantic Ocean leads us to suspect the steric contribution, especially the halosteric component, as the main contributor to the budget non-closure in this region, as the global budget without the North Atlantic region is closed within the error bars. Although we chose the SIO data set to estimate the steric component, considering that the salinity data had been corrected for the Argo floats instrumental drift that led to spurious salinity measurements, our study points to remaining errors affecting the halosteric component. Mu et al. (2024) also suggest a potential salinity bias in the Argo data set of the North Atlantic. Our results suggest that the salinity adjustment to the WOCE salinity climatology proposed by the SIO methodology may not fully correct for the rapid salinity drift experienced by some Argo floats. However, the different locations of the North Atlantic residual patterns when considering

https://doi.org/10.5194/egusphere-2024-3945
Preprint. Discussion started: 15 January 2025

the reanalyses or GRACE for the manometric component, as well as larger residuals in the northeast Atlantic Ocean in the GRACE case, suggest that uncertainty in GRACE data also plays a role. In other oceanic regions, some small-scale residual structures are observed, especially over western boundary currents and along the Antarctic circumpolar current. This may eventually result from differences in resolution of the gridded data sets used in this study, even though a low pass filter was applied to all data sets. .

The problem of the North Atlantic halosteric component highlighted in our regional budget study needs to be fixed up at the processing level of the Argo-based measurements. Our findings are helpful to the scientific groups involved in the Argo network as we can identify regions where the salinity contribution to regional sea level change appears to be spurious. This may help them in refining their investigations on the quality control checks to be applied to the Argo profiles. In addition, detailed investigation of the GRACE contribution to the residuals of this region should also be carried out in parallel. Our study highlights the necessity of applying consistent data processing and using similar reference systems for satellite altimetry and gravimetry data. Improved data should indeed be made available to the community, not only for sea level budget assessments but also for other applications in oceanography or climate-related research (i.e., for Earth's energy imbalance studies based on sea level budget approaches).

Acknowledgements

We thank the Magellium/LEGOS climate change team for providing us with the ensemble mean of the GRACE-based spherical harmonics solutions.

This research was carried out under a programme of, and funded by, the European Space Agency (ESA) Climate Change Initiative, within the project entitled "Sea level budget closure CCI+ (SLBC_CCI+)" (contract number 4000140620/23/I-BN).

Part of this work was performed in the context of the ERC Synergy GRACEFUL project (ERC Synergy grant n° 855677).

Authors contribution

Conceptualization : MB, AB, AC. Data analysis : MB, AB. Reanalysis computation: CY, AS. Writing original draft : AC. Writing, review and editing: all co-authors.

Conflict of interest

https://doi.org/10.5194/egusphere-2024-3945
Preprint. Discussion started: 15 January 2025

575 The authors declare no conflict of interest relevant to this study.

576 **References**

577 Ablain M., R. Jugier, L. Zawadki, and N. Taburet (2017). "The TOPEX-A Drift and Impacts on
578 GMSL Time Series." AVISO Website. October 2017.
579 https://meetings.aviso.altimetry.fr/fileadmin/user_upload/tx_ausyclsseminar/files/Poster_OST
580 ST17_GMSL_Drift_TOPEX-A.pdf.

581 Ablain, M., Meyssignac B., Zawadski, L., Jugler R., Ribes, A., Spada, G., Benveniste, J.,
582 Cazenave, A. and Picot, N. (2019), Uncertainty in satellite estimates of global mean sea-level
583 changes, trend and acceleration, *Earth Syst. Sci. Data*, 11, 1189–1202.

584 Adhikari, S., Ivins, E. R., Frederikse, T., Landerer, F. W., and Caron, L. (2019). Sea-level
585 fingerprints emergent from GRACE mission 573 data, *Earth Syst. Sci. Data*, 11, 629–646,
586 https://doi.org/10.5194/essd-11-629-2019.

587 Barnoud, A., Pfeffer, J., Cazenave, A., Fraudeau, R., Rousseau, V., & Ablain, M. (2023).
588 Revisiting the global mean ocean mass budget over 2005–2020. *Ocean Science*, 19, 321–
589 334, https://doi.org/10.5194/os-19-321-2023.

590 Barnoud A. et al. (2021). Contributions of altimetry and Argo to non-closure of the global
591 mean sea level budget since 2016, published online 26 June 2021, *Geophys. Res. Lett.*,
592 https://doi.org/10.1029/2021GL092824.

593 Blazquez A., Meyssignac B., Lemoine J.M., Berthier E., Ribes A. and Cazenave A. (2018).
594 Exploring the uncertainty in GRACE estimates of the mass redistributions at the Earth'
595 surface. Implications for the global water and sea level budgets, *Geophysical Journal*
596 *International*, 215(1), 415-430.

597 Blockley, E. W., Martin, M. J., McLaren, A. J., Ryan, A. G., Waters, J., Lea, D. J., Mirouze, I.,
598 Peterson, K. A., Sellar, A., and Storkey, D. (2014). Recent development of the Met Office
599 operational ocean forecasting system: an overview and assessment of the new Global
600 FOAM forecasts, *Geosci. Model Dev.*, 7, 2613–2638, https://doi.org/10.5194/gmd-7-2613-
601 2014.

602 Brown S, Willis J, Fournier S. (2023). Jason-3 wet path delay correction. Ver. F. PO.DAAC,
603 CA, USA. https://doi.org/10.5067/J3L2G-PDCOR.

604 Camargo C.M. et al. (2023). Regionalizing the sea level budget with machine learning
605 techniques, *Ocean Science*, 19, 17-41, https://doi.org/10.5194/os-19-17-2023.

606 Caron, L., Ivins, E. R., Larour, E., Adhikari, S., Nilsson, J., & Blewitt, G. (2018). GIA model
607 statistics for GRACE hydrology, cryosphere and ocean science. *Geophysical Research*
608 *Letters*, 45, 2203– 2212. https://doi.org/10.1002/2017GL07664.

609 Carrere L. and Lyard F. (2003), Modeling the barotropic response of the global ocean to
610 atmospheric wind and pressure forcing. Comparisons with observations. *Geophys. Res. Lett.*
611 30, 6, 1275, https://doi.org/10.1029/2002GL016473.

612 Carret, A., Llovel, W., Penduff, T., & Molines, J.-M. (2021). Atmospherically forced and chaotic
613 interannual variability of regional sea level and its components over 1993–2015. *Journal of*
614 *Geophysical Research: Oceans*, 126, e2020JC017123.
615 https://doi.org/10.1029/2020JC017123

https://doi.org/10.5194/egusphere-2024-3945
Preprint. Discussion started: 15 January 2025

Carret A., Johannessen J., Andersen O., Ablain M., Prandi P., Blazquez A. and Cazenave A. (2017). Arctic sea level during the altimetry era, Surveys in Geophysics, 38, 251-277, https://doi.org/10.1007/s10712-016-9390-2.

Carton, J. A., G. A. Chepurin, and L. Chen (2018). SODA3: A New Ocean Climate Reanalysis. *J. Climate*, 31, 6967–6983, https://doi.org/10.1175/JCLI-D-18-0149.1.

Cazenave A., Palanisamy H. and Ablain M. (2018). Contemporary sea level changes from satellite altimetry: What have we learned? What are the new challenges? *Advances in Space Research*, https://doi.org/10.1016/j.asr.2018.07.017, published online 27 July 2018.

Cazenave A. and Moreira L. (2022). Contemporary sea level changes from global to local scales: a review, *Proc. Royal Society*, 478, 20220049. https://doi.org/10.1098/rspa.2022.0049.

Chen, J.L., Tapley, B. D., Save, H., Tamisiea, M. E., Bettadpur, S., & Ries, J. (2018). Quantification of ocean mass change using gravity recovery and climate experiment, satellite altimeter, and Argo floats observations. *Journal of Geophysical Research: Solid Earth*, 123, 10,212–10,225. https://doi.org/10.1029/2018JB016095.

Chen J.L., Tapley B.D., Seo K-W., Wilson C. and Ries J. (2019), Improved Quantification of Global Mean Ocean Mass Change Using GRACE Satellite Gravimetry Measurements ». *Geophysical Research Letters* 46, 23, 13984- 91. https://doi.org/10.1029/2019GL085519.

Chen J.L., Tapley B.D., Wilson C., Cazenave A., Seo K-W. and Kim J.S. (2020). Global ocean mass change from GRACE 1 and GRACE Follow-On, and altimeter and Argo measurements, *Geophys. Res. Lett*., https://doi.org/10.1029/2020GL090656, published online, 3 November 2020.

Dangendorf S, Frederikse T, Chafik L, Klinck JM, Ezer T, Hamlington BD. (2021). Data-driven reconstruction reveals large-scale ocean circulation control on coastal sea level. *Nat. Clim.Change* 11, 514–520. https://doi.org/10.1038/s41558-021-01046-1.

Dieng H.B., Cazenave A., Meyssignac B. and Ablain M. (2017). New estimate of the current rate of sea level rise from a sea level budget approach, *Geophys. Res. Lett*., 44, https://doi/org/10.1002/2017GL073308.

England, M.H., McGregor, S., Spence, P., Meehl, G. A. (2014). Recent intensification of wind-driven circulation in the Pacific and the ongoing warming hiatus. *Nature Climate Change*, **4**, 222-227, https://doi.org/10.1038/NCLIMATE2106.

Flechtner, F., Dobslaw, H. & Fagiolini, E. (2015). AOD1B Product Descrip tion Document for Product Release 05 Rev4.4 GRACE 327–750, Geo Forschungszentrum Potsdam, Potsdam, Germany.

Forget, G., and Ponte, R. M. (2015). The partition of regional sea level variability. *Progr. Oceanogr*. 137, 173–195. https://doi.org/10.1016/j.pocean.2015.06.002.

Frederikse, T., Riva, R., Kleinherenbrink, M., Wada, Y., den Broeke, M. van, and Marzeion, B. (2016), Closing the sea level budget on a regional scale: Trends and variability on the Northwestern European continental shelf, *Geophys. Res. Lett*., 43, 10,864– 10,872, https://doi.org/10.1002/2016GL070750.

https://doi.org/10.5194/egusphere-2024-3945
Preprint. Discussion started: 15 January 2025

Frederikse, T., Jevrejeva, S., Riva, R. E. M., & Dangendorf, S. (2018). A Consistent Sea-Level Reconstruction and Its Budget on Basin and Global Scales over 1958–2014, *Journal of Climate*, 31(3), 1267-1280. Retrieved Mar 29, 2022, from https://journals.ametsoc.org/view/journals/clim/31/3/jcli-d-17-0502.1.xml.

Frederikse T et al. (2020). The causes of sea-level rise since 1900. *Nature* 584, 393–397, https://doi.org/10.1038/s41586-020-2591-3.

Garric, G., and Parent, L. (2017). Quality Information Document for Global 1330 Ocean Reanalysis Products Global-Reanalysis-Phy-001-025. Available online at: https://catalogue.marine.copernicus.eu/documents/QUID/CMEMS-GLO-QUID-001-025.pdf

Gregory, J. M. & Lowe, J. A. (2000). Predictions of global and regional sea- level rise using AOGCMs with and without flux adjustment. *Geophysical Research Letters*, 27(19), 3069-3072. https://doi.org/10.1029/1999GL011228.

Gregory J.M. et al. (2019). Concepts and Terminology for Sea Level: Mean, Variability and Change, Both Local and Global, *Surveys in Geophysics*, 40:1251–1289, https://doi.org/10.1007/s10712-019-09525-z.

Guérou, A., Meyssignac, B., Prandi, P., Ablain, M., Ribes, A., and Bignalet-Cazalet, F. (2023). Current observed global mean sea level rise and acceleration estimated from satellite altimetry and the associated measurement uncertainty, *Ocean Sci.,* 19, 431–451, https://doi.org/10.5194/os-19-431-2023.

Hamlington et al. (2020). Undertstanding contemporary regional sea level change and the implications for the future, *Review of Geophysics*, https://doi.org/10.1029/2019RG000672.

Hamlington, B. D., Cheon, S. H., Piecuch, C. G., Karnauskas, K. B., Thompson, P. R., Kim, K.- Y., et al. (2019). The dominant global modes of recent internal sea level variability. *Journal of Geophysical Research: Oceans*, 124, 2750–2768. https://doi.org/10.1029/2018JC014635.

Han, W., Meehl, G., Stammer, D., Hu, A., Hamlington, B., Kenigson, J., et al. (2017). Spatial patterns of sea level variability associated with natural internal climate modes. *Surveys in Geophysics*, 38(1), 217–250. https://doi.org/10.1007/s10712- 016- 9386- y.

Han W., Stammer D., Thompson P., Ezer T., Palanisamy H., Zhang X., Domingues C., Zhang L., Yuan D., (2019). Impacts of Basin- Scale Climate Modes on Coastal Sea Level: a Review, *Surveys in Geophysics*, 40, 1493–1541, https://doi.org/10.1007/s10712-019-09562-8.

Horwath M., Gutknetch B., Cazenave A., et al., (2022). Global sea level budget and ocean mass budget, with focus on advanced data products and uncertainty characterization. *Earth System Science Data*, 14, 411–447, 2022 https://doi.org/10.5194/essd-14-411-2022.

IPCC (2019). IPCC Special Report on the Ocean and Cryosphere in a Changing Climate, edited by Portner, H.-O., Roberts, D. C., Masson-Delmotte, V., Zhai, P., Tignor, M., Poloczanska, E., Mintenbeck, K., Alegriìa, A., Nicolai, M., Okem, A., Petzold, J., Rama, B., and Weyer, N. M.

IPCC (2021), Climate Change 2021. The Physical Science Basis. Contribution of Working Group I to the Sixth Assessment Report of the Intergovernmental Panel on Climate Change [Masson-Delmotte, V., P. Zhai, A. Pirani, S.L. Connors, C. Péan, S. Berger, N. Caud, Y. Chen, L. Goldfarb, M.I. Gomis, M. Huang, K. Leitzell, E. Lonnoy, J.B.R. Matthews, T.K. Maycock, T. Waterfield, O. Yelekçi, R. Yu, and B. Zhou (eds.)]. Cambridge University Press. In Press.

https://doi.org/10.5194/egusphere-2024-3945
Preprint. Discussion started: 15 January 2025

699 Llovel, W., and T. Lee (2015), Importance and origin of halosteric contribution to sea level
700 change in the southeast Indian Ocean during 2005–2013, *Geophys. Res. Lett.*, 42, 1148–
701 1157, https://doi.org/10.1002/2014GL062611.

702 Llovel, W., Balem, K., Tajouri, S., & Hochet, A. (2023). Cause of substantial global mean sea
703 level rise over 2014–2016. *Geophysical Research Letters*, 50, e2023GL104709.
704 https://doi.org/10.1029/2023GL104709.

705 Loomis, B. D., Luthcke, S. B., & Sabaka, T. J. (2019). Regularization and error characterization
706 of GRACE mascons. *Journal of Geodesy*, 93(9), 1381–1398. https://doi.org/10.1007/s00190-
707 019-01252-y.

708 Lorbacher, K., Marsland, S. J., Church, J. A., Griffies, S. M., Stammer, D. (2012). Rapid
709 barotropic sea level rise from ice sheet melting. *Journal of Geophysical Research*, 117,
710 C06003, https://doi.org/10.1029/2011JC007733.

711 Liu C., Liang X., Ponte R.M.. and Chambers D.P. (2020). Global patterns of spatial and
712 temporal variability in multiple gridded salinity products, *J. Climate*, 33, 20, 8751-8766,
713 https://doi.org/10.1175/jcli-d-20-0053.1.

714 Liu C., Liang X., Ponte R.M. and Chambers D.P. (2024). 3Salty Drifts" of argo floats affects
715 the gridded ocean salinity products, *J. Geophys. Res. -Oceans*, 129, c2023JC020871,
716 https://doi.org/10.1019/2023JC020871.

717 Ludwigsen C.B. et al. (2024). Global and regional ocean mass budget closure since 2003,
718 Nature Communications, 15, 1416, https://doi.org/10.1038/s41467-024-45726-w.

719 Ludwigsen C.B., Andersen O.B. and rose S.K. (2022), Components of 20 years (1995-2015)
720 of absolute sea level trends in the Arctic, *Ocean Science*, 181,109-127,
721 https://doi.org/10.5194/os-18-109-2022.

722 Merrifield, M. A., and Maltrud, M. E. (2011), Regional sea level trends due to a Pacific trade
723 wind intensification, *Geophys. Res. Lett.*, 38, L21605, https://doi.org/10.1029/2011GL049576.

724 Milne G.A., Gehrels W.R., Hughes C.W. and Tamisea M.E. (2009), Identifying the causes of
725 sea level change, *Nature Geosci* 2, 471–478. https://doi.org/10.1038/ngeo544.

726 Mitrovica J, Tamisiea ME, Davis JL, Milne GA. (2001). Recent mass balance of polar ice
727 sheets inferred from patterns of global sea-level change. *Nature,* 409, 1026–1029,
728 https://doi.org/10.1038/35059054.

729 Mu D., Church J.A., King M., Ludwigsen C.B. and Xu T. (2024). Contrasting discrepancy in
730 the sea level budget between the North and South Atlantic Ocean since 2016, *Earth and*
731 *Space Science,* 11, e2023EA003133, https://doi.org/10.1029/2023EA003133.

732 Nerem, R.S., Beckley, B.D., Fasullo, J., Hamlington, B.D., Masters, D. and Mitchum, G.T.
733 (2018). Climate Change Driven Accelerated Sea Level Rise Detected In The Altimeter Era,
734 *Proceedings of the National Academy of Sciences,* 15, 9, 2022-2025,
735 https://doi.org/10.1073/pnas.1717312115.

736 Peltier R.W. (2004), Global Glacial Isostasy and the Surface of the Ice-Age Earth: The ICE-
737 5G (VM2) Model and GRACE, Annual Review of Earth and Planetary Science, 32, 111-149.

https://doi.org/10.5194/egusphere-2024-3945
Preprint. Discussion started: 15 January 2025

738 Peltier R.W., D. F. Argus, and R. Drummond (2018). "Comment on “An assessment of the
739 ICE- 6G_C (VM5a) glacial isostatic adjustment model” by Purcell et al." *Journal of*
740 *Geophysical Research- Solid Earth* 123, 2, 2019-2028.

741 Piecuch CG and Ponte RM. (2014). Mechanisms of global mean steric sea level change. *J.*
742 *Clim.* 27, 824–834, https://doi.org/10.1175/JCLI-D-13-00373.1.

743 Ponte R.M., Sun Q., Liu C. and Liang X. (2021). How salty is the global ocean: weighting it all
744 or tasting it a sip at a time, *Geophys. Res. Lett.*, 48, 11, e2021GL092935,
745 https://doi.org/10.1029/2021gl092935.

746 Prandi, P., Meyssignac, B., Ablain, M. et al. (2021). Local sea level trends, accelerations and
747 uncertainties over 1993–2019. *Nature Sci Data*, 626, 8, 1. https://doi.org/10.1038/s41597-020-
748 00786-7.

749 Proshutinsky AIM, Ashik EN, Dvorkin S, Häkkinen RA, Krishfield PWR. (2004). Secular sea
750 level change in the Russian sector of the Arctic Ocean. *J. Geophys. Res*. 109, C03042,
751 https://doi.org/10.1029/2003JC002007.

752 Purkey SG, Johnson GC. (2010). Warming of Global Abyssal and Deep Southern Ocean
753 Waters between the 1990 s and 2000 s, contributions to Global Heat and Sea Level Rise
754 Budgets. *J. Clim.* 23, 6336–6351, https://doi.org/10.1175/2010JCLI3682.1.

755 Rietbroek, R., Brunnabend, S. E., Kusche, J., Schröter, J., and Dahle, C. (2016). Revisiting
756 the contemporary sea-level budget on global and regional scales. *Proc. Natl. Acad. Sci*., 113,
757 1504–1509. https://doi.org/10.1073/pnas.1519132113.

758 Roberts CD, Calvert D, Dunstone N, Hermanson L, Palmer MD, Smith D. (2016). On the
759 drivers and predictability of seasonal to interannual variations in regional sea level. J. Clim.
760 29, 7565–7583, https://doi.org/10.1175/JCLID-D-15-0886.1.

761 Roemmich D, Gilson J. (2009). The 2004–2008 mean and annual cycle of temperature,
762 salinity, and steric height in the global ocean from the Argo Program. *Prog. Oceanogr.* 82, 81–
763 100, https://doi.org/10.1016/j.pocean.2009.03.004.

764 Royston, S., Vishwakarma, B. D., Westaway, R. M., Rougier, J., Sha, Z., and Bamber, J. L.
765 (2020). Can we resolve the basin-scale sea level 557 trend budget from GRACE ocean mass?
766 *Journal of Geophysical Research- Oceans*, 125, e2019JC015535. 558,
767 https://doi.org/10.1029/2019JC015535.

768 Save H., Bettadpur S. and Tapley B.D. (2016). High resolution CSR GRACE RL05 mascons,
769 *J. Geophys. Res. Solid Earth*, 121, 7547-7569, https://doi.org/10.1002/2016jB013007.

770 Spada, G. (2017). Glacial isostatic adjustment and contemporary sea level rise: An overview.
771 *Surveys in Geophysics*, 38, 153- 587 185. https://doi.org/10.1007/s10712-016-9379-x.

772 Sun, Y., Riva, R., & Ditmar, P. (2016). Optimizing estimates of annual variations and trends in
773 geocenter motion and J2 from a combination of GRACE data and geophysical models. *Journal*
774 *of Geophysical Research,* 121(11), 8352-8370. https://doi.org/10.1002/2016JB013073.

775 Stammer D., Cazenave A., Ponte R. M., Tamisiea M. E. (2013). Causes for contemporary
776 regional sea level changes. *Ann Rev Mar Sci.* 567, 5, 21- 46. https://doi.org/10.1146/annurev-
777 marine-121211-172406.

https://doi.org/10.5194/egusphere-2024-3945
Preprint. Discussion started: 15 January 2025

778 Storto, A. and Masina, S (2016). C-GLORSv5: an improved multipurpose global ocean eddy-
779 permitting physical reanalysis, *Earth Syst. Sci. Data*, 8, 679–696, https://doi.org/10.5194/essd-
780 8-679-2016.

781 Storto, A., Yang, C. (2024). Acceleration of the ocean warming from 1961 to 2022 unveiled by
782 large-ensemble reanalyses. *Nat Commun* 15, 54(, https://doi.org/10.1038/s41467-024-44749-
783 7.

784 Storto, A., Chierici, G., Pfeffer, J., Barnoud, A., Bourdalle-Badie, R., Blazquez, A., Cavaliere,
785 D., Lalau, N., Coupry, B., Drevillon, M., Fourest, S., Larnicol, G., and Yang, C. (2024).
786 Variability in manometric sea level from reanalyses and observation-based products over the
787 Arctic and North Atlantic oceans and the Mediterranean Sea, in: 8th edition of the Copernicus
788 Ocean State Report (OSR8), edited by: von Schuckmann, K., Moreira, L., Grégoire, M.,
789 Marcos, M., Staneva, J., Brasseur, P., Garric, G., Lionello, P., Karstensen, J., and
790 Neukermans, G., Copernicus Publications, State Planet, 4-osr8, 12,
791 https://doi.org/10.5194/sp-4-osr8-12-2024.

792 Swenson, S., Chambers, D., & Wahr, J. (2008). Estimating geocenter variations from a
793 combination of GRACE and ocean model output. *Journal of Geophysical Research*, 113, B8410.
794 https://doi.org/10.1029/2007JB005338.

795 Tamisiea, M. E. (2011). Ongoing glacial isostatic contributions to observations of sea level
796 change. *Geophys. J. Int*. 186, 1036–1044. https://doi.org/10.1111/j.1365-246X.2011.05116.x.

797 Tajouri S., W. Llovel, F. Sévellec, J.M. Molines, P. Mathiot, et al. (2024). Simulated Impact of
798 Time-Varying River Runoff and Greenland Freshwater Discharge on Sea Level Variability in
799 the Beaufort Gyre Over 2005–2018. *Journal of Geophysical Research. Oceans*, 129, 9,
800 https://doi.org/10.1029/2024JC021237.

801 Tapley, B., Watkins, M. M., Flechtner, F., Reigber, C. et al. (2019). Contributions of GRACE
802 to understanding climate change, *Nature Climate Change*, 9, 358–369.
803 https://doi.org/10.1038/s41558-019-0456-2.

804 Timmermann, A., McGregor, S., Jin, F. -F. (2010), Wind effects on past and future regional
805 sea level trends in the southern Indo-Pacific. *Journal of Clim*ate, **23**(16), 4429–4437,
806 https://doi.org/10.1175/2010JCLI3519.1.

807 Wang O., Lee T., Piecuch C.G., Fukumori I., Fenty I., Frederiske T. et al. (2022). Local and
808 remote forcing of interannual sea level variability at Nantucket Island, *J. Geophys. Res.*
809 *Oceans*, 127, 6,e2021JC018275, https://doi.org/10.1029/2021jc018275.

810 Watkins, M. M., Wiese, D. N., Yuan, D.-N., Boening, C., & Landerer, F. W. (2015). Improved
811 methods for observing Earth's time variable mass distribution with GRACE using spherical cap
812 mascons. *Journal of Geophysical Research: Solid Earth,* 120, 2648–2671.
813 https://doi.org/10.1002/2014JB011547.

814 WCRP Global Sea Level Budget Group (The) (2018). Global sea level budget, 1993-present,
815 *Earth System Science Data*, 10, 1551-1590, https://doi.org/10.5194/essd-10-1551-2018.

816 Wong A., Gilson J. and Cabanes C. (2023). Argo salinity: bias and uncertainty evaluation,
817 *Earth Syst. Sci.data*, 15, 383-393, https://doi.org/10.5194/essd-15-383-2023.

818 Wunsch C and Stammer D. (1997). Atmospheric loading and the oceanic 'inverted barometer'
819 effect. *Rev. Geophys*. 35, 79–107, https://doi.org/10.1029/96RG03037.

https://doi.org/10.5194/egusphere-2024-3945
Preprint. Discussion started: 15 January 2025

820 Zuo H., Balmaseda M.A., Tietsche S., Mogensen K., Mayer M. (2019), The ECMWF
821 operational ensemble reanalysis–analysis system for ocean and sea ice: A description of the
822 system and assessment. *Ocean Sci.* 15, 779–808.